Journal of Research and Applications in Mechanical Engineering
ISSN: 2229-2152 (Print); 2697-424x (Online)
(2025) Vol. 13, No. 3, Paper No. JRAME 25-13-044
[DOI: 10.14456/ jrame.2025.44]

Research Article

Investigating PEMFC Performance with Dead-Ended Anode and Pressure Swing Technique under Dynamic Loading

D. P. Doan[1]
V. Lilavivat[2,*]
T. Sasabe[3]
C. T. Vo[4]
T. D. Pham[1]
K. H. Nguyen[1]
C. Charoenphonphanich[1]
[1] Department of Mechanical Engineering, School of Engineering, King Mongkut's Institute of Tecnhnology Ladkrabang, Bangkok, 10520, Thailand
[2] National Energy Technology Center, National Science and Technology Development Agency, Pathum Thani, 12120, Thailand
[3] School of Engineering, Tokyo Institute of Technology, Tokyo, 152-8552, Japan
[4] Faculty of Automotive Engineering Technology, Faculty of Engineering, Industrial University of Ho Chi Minh City, Ho Chi Minh City 727900, Vietnam

Received 30 August 2024
Revised 27 December 2024
Accepted 4 January 2025

Abstract:
The anode water management is a significant factor to mitigate local flooding and enhance performance at Proton Exchange Membrane Fuel Cells (PEMFC). The Dead-end anode (DEA) configuration operates dry hydrogen and utilizes a solenoid valve to seal the anode outlet. The Pressure Swing Technique (PST), based on the DEA configuration, generates periodic flow by adding more hydrogen via a solenoid valve between the inlet and outlet lines, rather than solely using a solenoid valve at the anode outlet. The hysteresis phenomenon, observed through dynamic voltage transients during forward and backward current sweeps, is applied in this study to investigate performance through voltage difference, voltage change, voltage decay rate, and voltage stability index under DEA and PST configurations in a single cell. The results indicated that PST improved stability by redistributing water within the anode channel but exhibited lower power density, specifically 5.46% less at a high current density of 400 mA cm^{-2} *due to insufficient membrane hydration. Additionally, longer purging intervals decreased cell output voltage while gradually enhancing stability for both configurations. Furthermore, slower switching period rates in PST leaded to instability.*

Keywords: *PEMFC, Dead-ended anode, Pressure swing technique, Dynamic voltage, Periodic pulsation*

1. Introduction

Proton Exchange Membrane Fuel Cells (PEMFCs) represent a highly promising alternative to internal combustion engines, primarily due to their high efficiency and low emissions. PEMFCs generate electricity by facilitating an electrochemical reaction between hydrogen and oxygen, producing only water and heat as by-products, which positions them as a leading clean energy technology [1]. These have attracted significant attention because of their potential to support achieving net zero emissions by 2050 [2]. However, this technology faces substantial challenges related to the cost of equipment, fuel, and the durability of the membrane electrode assembly (MEA) [3]. Previous studies have explored the use of recirculation systems, unreacted fuel is recirculated upstream along with fresh hydrogen. Consequently, this approach complicates the system and increases costs [4-7].

In contrast, the DEA configuration uses a solenoid valve at the outlet channel instead of a recirculation system to maintain the reactant flow, simplifying the system while significantly enhancing hydrogen utilization compared to the flow-through configuration [6, 8]. However, water diffusion from the cathode to the anode accumulates gradually downstream when the solenoid valve is closed, leading to flooding and voltage loss [9, 10]. This issue trigger a

---

* Corresponding author: V. Lilavivat
E-mail address: visarn.lil@entec.or.th

series of significant problems. For example, Meyer et al. [11] and Hu et al. [12] pointed out that flooding was caused not only by water diffusion but also by nitrogen, which prevented hydrogen from reaching the reaction area, leading to hydrogen starvation downstream. Yu et al. [13] found that local fuel starvation results in high cathode potential, accelerating carbon corrosion, especially downstream, causing irreversible performance decline. Many researchers [14-16] concurred with these findings. Matsuura et al. [17] discovered that repeated purging valve processes with low cathode humidity cause membrane pin-holes, combined with uneven mechanical stress leading to membrane cracks upstream, both contributing to accelerated mechanical damage. Therefore, the water management within anode channel is crucial for optimizing the efficiency of the DEA configuration.

In recent years, efforts to enhance water management have led to significant improvements in the DEA configuration by modifying the hydrogen feed method. A solenoid valve was introduced before the anode outlet to reverse hydrogen back into the anode channel, generating a fluctuating flow that improves cell performance [18-27]. Specifically, Zhao et al. [22-24] conducted experiments with this new configuration on stacks using visualization techniques. Their findings revealed that employing the proposed method resulted in a slower rate of voltage decay, enhanced cell stability, more effective water distribution, and significantly improved performance at high current densities compared to the conventional DEA. In the latest three-dimensional study [27], the water saturation of the gas diffusion layer (GDL) decreased by 31%, and the time-averaged diffusion coefficient of hydrogen increased by 14%. Yang et al. [19, 25] applied scanning electron microscope (SEM) imaging techniques to experimentally compare local degradation phenomena under the new configuration and DEA convection. The efficiency elimination of flooding indicated that thickness reductions in the cathode catalyst layer (CL) and membrane were significantly mitigated in downstream and upstream areas, respectively.

In this study, a single cell was utilized to compare water management between the DEA and PST configurations under dynamic loading. Although the the valve control methods are similar to previous studies, the different in number of cells (listed in Table 1) leads to significant differences in water management results. A single cell was chosen for its suitability in implementing advanced imaging techniques, such as SEM, to examine the durability of the membrane and catalyst layer in detail. In contrast, applying SEM to a cell stack introduces significant complexity and cost, which can compromise the feasibility of the study. The findings will provide key insights into water management under dynamic loading, with a specific focus on the PST configuration in a single cell setup, a novel area that has yet to be addressed in the current research. These insights will form a basis for scaling up PEMFC systems with improved efficiency and durability.

Table 1: The previous studies applying the PST configuration to improve PEMFC performance.

Test PEMFC system	**Performance improvement**	**Ref.**
40 cells stack, parallel flow field, active area 68.5 cm^2	Improved PEMFC stack performance by 13.7% at 365 mA cm^{-2}	[21]
10 cells stack, parallel flow field, active area 62 cm^2	Improved voltage decay characteristics more than total output power at high currents	[23]
4 cells stack, parallel flow field, active area 13 cm^2	Enhanced the transport of water droplets and effectively inhibits condensation of water vapor	[24]
20 cells stack, parallel flow filed, active area 18 cm^2	Nearly 100% utilization rate of hydrogen was achieved.	[28]
10 cells stack, parallel flow field, active area 62 cm^2	The maximum power of the stack increased by 7.71% at 700 mA cm^{-2}	[26]

2. Experimental

2.1 Experimental system

In this study, the membrane electrode assembly (MEA) has an active area of 25 cm², using a decal MEA coated on two pieces of carbon paper with electrode catalysts. The platinum electro-catalyst loading is 0.32 mg cm^{-2} at the cathode and 0.1 mg cm^{-2} at the anode. A single cell with a pair of bipolar plates featuring a triple serpentine flow channel is employed, with reactant gas flowing in a co-flow configuration. To prevent the gravitational effect on the results, the gas flow inside the cell must move parallel to the horizontal plane.

As shown in Fig. 1a, the experimental setup includes gas supply system and a data acquisition system. At the anode channel, dry hydrogen (99.999%) is depressurized by a pressure regulator before being directed through to the cell. At the cathode side, the air is supplied to the cell through a mass flow controller and a humidifier. The outlet voltage is measured by E-load, which then sent signals to the control interface. It manages the output parameters and records the values with a sampling rate of 200 ms, programmed using LabVIEW from National Instruments. The microcontroller unit is used to control solenoid valves and transmit data to the control interface.

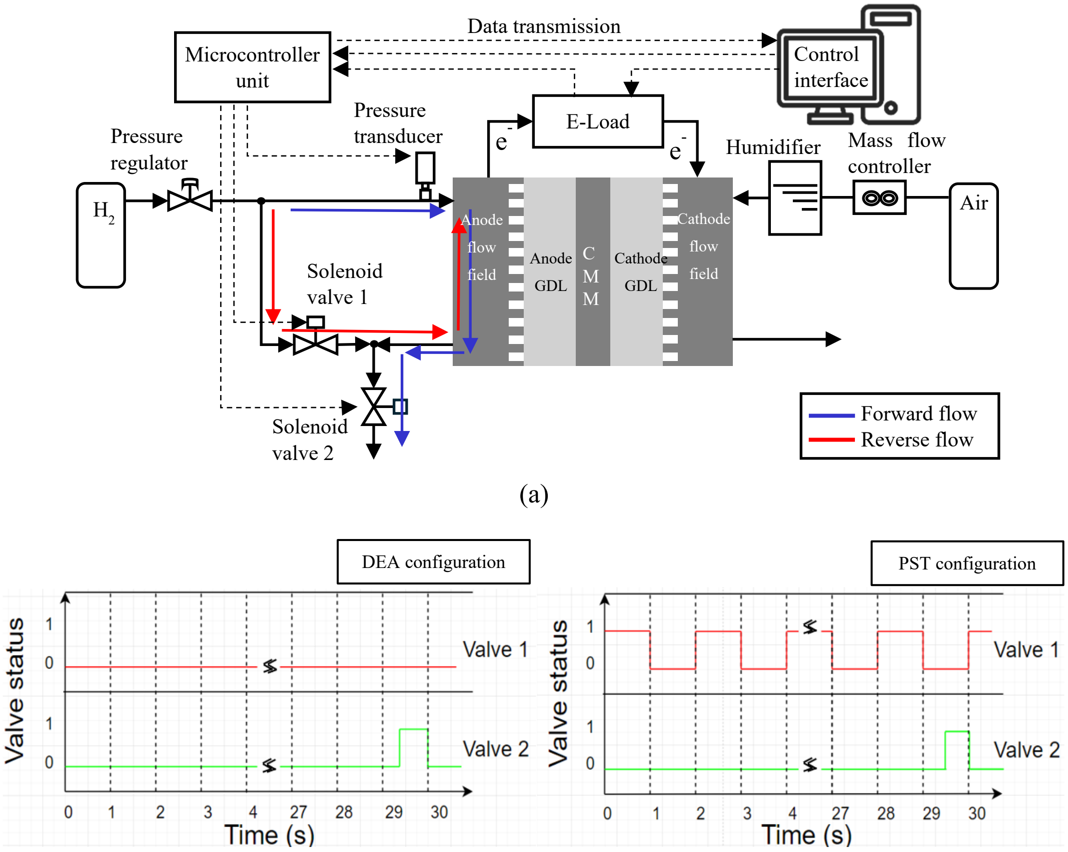

(a)

(b)

Fig. 1. Experiment setup for the PEMFC: (a) The PEMFC testing system diagram; (b) The operating chart of solenoid valves in DEA configuration and PST configuration.

2.2 Experimental setup

To ensure the experimental results are repetitive and stable, the membrane is fully activated. Afterward, excess water in the cell is purged to ensure consistent initial operating conditions for each experiment. During the process, the hydrogen inlet is regulated at 0.7 bar and the temperature is maintained at 60 ^{o}C, the relative humidity (RH) and stoichiometric air ratio are maintained at 100% and 2.5, respectively.

Hysteresis phenomenon indicates dynamic behaviour by forward sweeping and backward current, enabling the evaluation of material properties and operating conditions. The current is swept from OCV to 10 A and then backward to OCV with each step incrementing by 2 A over 5 mins. However, the voltage valves are recorded during the last 200 s of each current level due to the instability of cell voltage when the current suddenly changes. In this experiment, the purging interval and duration are set consistently at 29.4 s and 0.6 s, respectively, for both configurations, with the valve control strategy shown in Fig. 1b. The purging interval is the period between each purge. During this interval, hydrogen only flows through the inlet channel in the DEA configuration. In the PST configuration, hydrogen is supplied not only through the inlet channel but also through the outlet channel via solenoid valve 1, creating a fluctuating flow within the cell. During the purging duration, the solenoid valve is opened, pushing the accumulated water out of the cell due to the pressure difference between the cell and the environment. The cell voltage is recovered immediately. The operating conditions are summarized in Table 2. Additionally, the PEMFC performance is investigated by varying the switching period rate of the PST configuration and the purging interval for both configurations at 320 mA cm^{-2}. In this study, the parameters of voltage difference, voltage change, voltage decay rate and voltage stability index are focused on to evaluate the cell performance. They are described as follows:

$$\text{Voltage difference} = \frac{V_{j,\text{backward}} - V_{j,\text{forward}}}{V_{j,\text{forward}}} * 100 \tag{1}$$

$$\text{Voltage change (i)} = V(i)_{\text{max,after purge}} - V(i)_{\text{min,during purge}} \tag{2}$$

$$\text{Voltage decay rate (i + 1)} = \frac{V(i)_{\text{max,after purge}} - V(i+1)_{\text{min,before purge}}}{T_1} \tag{3}$$

$$\text{Voltage stability index} = \sqrt{\frac{\int_{t_0}^{t_1}\left(\frac{V(t)-\overline{V}}{\overline{V}}\right)^2 dt}{\int_{t_0}^{t_1} dt}} \tag{4}$$

Where $V_{j,\text{forward}}$ and $V_{j,\text{backward}}$ represent the average voltage at the current density level j during the forward and backward sweeps, respectively. $V(i)_{\text{max,after purge}}$ and $V(i+1)_{\text{min,before purge}}$ are maximum voltage after the i-th purge and minimum voltage before the (i+1)-th purge, respectively; $V(i)_{\text{min,during purge}}$ is minimum value during the i-th purge; T_1 represents the purge interval of valve 2; $V(t)$ is the transient voltage at time t and $\overline{V}$ is average voltage from t_0 to t_1.

Table 2: Experiment conditions of the PEMFC

Conditions	Value
Cell temperature	60 ºC
Air humidity	100%
Air stoichiometric	2.5
Hydrogen inlet pressure	0.7 bar
Purging interval	4, 10, 18, 30, 60, 90 s
Purging duration	0.6 s
Switching period rate	1:1, 2.75:1, 5:1, 6.5:1, 9:1
Current density	0, 80, 160, 240, 320, 400 mA cm^{-2}
Duration each step	5 mins

3. Results and discussions

3.1 Comparing the performance of DEA and PST

The performance of DEA and PST was initially assessed under dynamic load conditions, with a current step duration of 5 mins. The hydrogen pressure was maintained at 0.7 bar for both configurations, and the switching period rate for PST was set to 1:1. The result of the performance are shown in Fig. 2a. During the low current densities forward sweep, electrochemical reactions intensity on the cathode side is weak, less water production. The water back diffusion effect from the cathode to the anode side is not significant while water molecules move from the anode to the cathode by electro-osmotic drag, the membrane is difficult to get hydrate condition, as supported by previous studies [10, 26]. There is no significant difference in performance between DEA and PST. During the higher current density, the electrochemical intensity is stronger, leading to increased water production on the cathode side and more vapor condensation on the anode side due to the back diffusion of water. At this point, the water management strategies of both configurations begin to differ clearly. The results depicted in Fig. 2b indicate that the power density of the PST configuration is lower than that of the DEA configuration at high current densities. Notably, at a current density of 400 mA cm^{-2}, the power density for the PST configuration is 5.46% lower than that of the DEA configuration. This result is contrary to the results of other authors, the cause apparently come from the difference in testing equipment, as shown in Table 1.

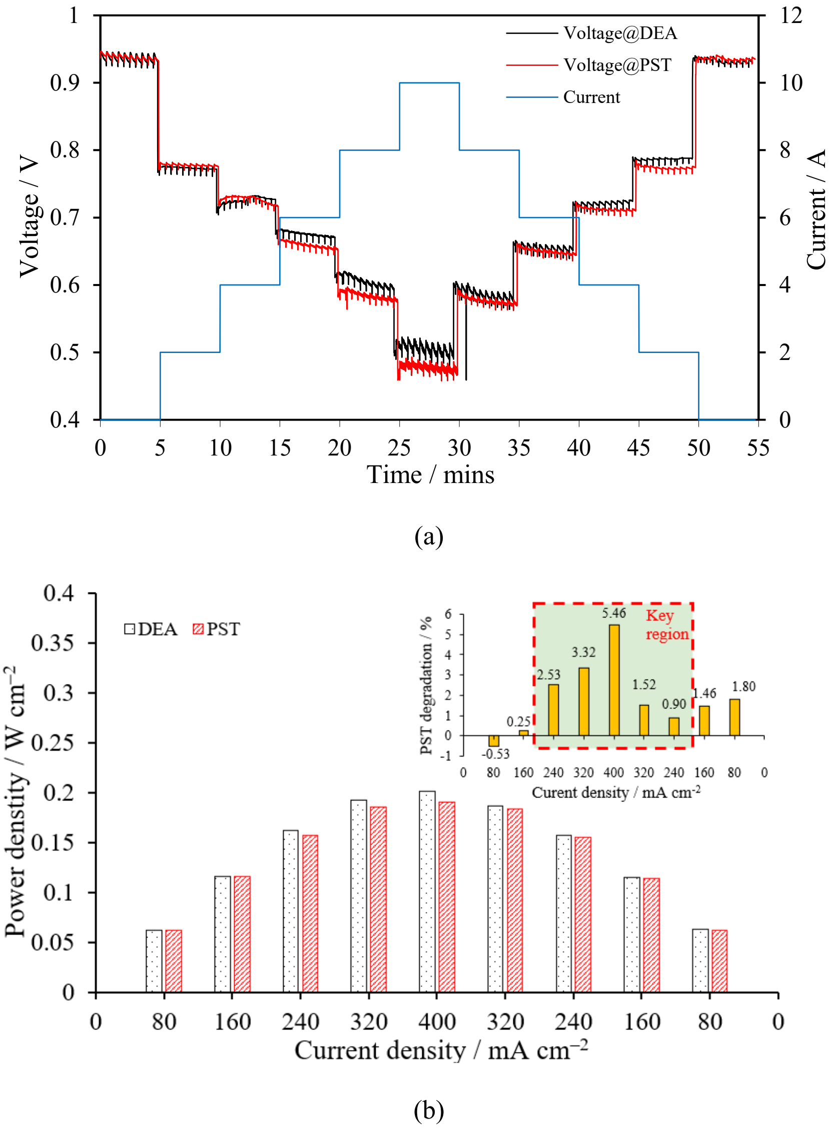

Fig. 2. The comparison of PEMFC performance with two different configuration under dynamic load: (a) The voltage evolution; (b) The power density.

For the DEA configuration, water vapor diffuses through the membrane, but the water production from the oxygen reduction reaction (ORR) in a single cell is lower compared to a stack. This results in the formation of droplets rather than local flooding, which block the GDL pores and prevent hydrogen from reaching the platinum surface of CL in the downstream. Conversely, in the PST configuration, water is redistributed in the midstream due to the effect of reverse flow, alleviating membrane dehydration in the upstream compared to DEA. However, this also increases the water concentration across the entire anode channel, reducing the water concentration gradient between the anode and cathode, leading to weaker back diffusion. Consequently, the membrane becomes more dehydrated, reducing ion conductivity, increasing ohmic resistance, and causing decreased voltage seriously.

The voltage difference indicates improvement voltage after the backward sweep compared to the same current level during the forward sweep. Notably, larger negative values indicate more severe water management issues, with greater flooding. During the backward sweep, continuous water production at high current densities, combined with residual water from the forward sweep, causes temporary flooding in both configurations, The DEA configuration shows significant voltage differences of -2.93% and -3% at 240 and 320 mA cm^{-2}, respectively, resulting in increased ohmic resistance and more pronounced voltage drops, as shown in Fig. 3. Conversely, the membrane remains better hydrated compared to the forward sweep and produces less water at low current densities, resulting in a slight improvement in DEA voltage, with a voltage difference of 1.8% at 80 mA cm^{-2}, while the PST voltage remains stable, voltage difference is lower by -0.6% at 80 mA cm^{-2} and at OCV.

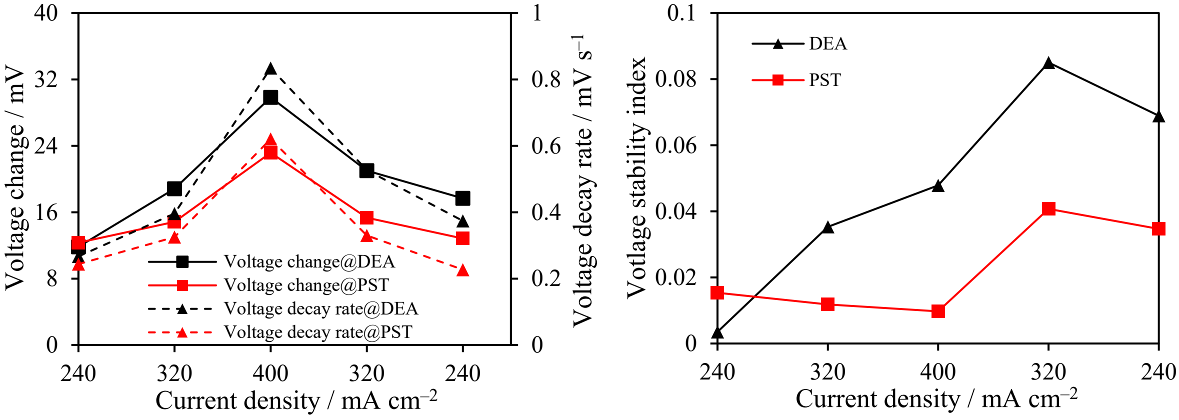

Fig. 3. Polarization curves under hyperesis phenomena.

Voltage change represents the variation in voltage during the purging of impurities through solenoid valve 2. A larger voltage change indicates more droplets are condensing, clogging the pores of the GDL, and potentially causing local flooding. The voltage decay rate is defined as the average voltage drop per second during each purge period of valve 2. Because the amount of water produced at low current densities is very low, there are no significant performance differences between the two configurations. Therefore, voltage change, voltage decay rate, and voltage stability index are only examined at high current densities (indicated by the green region in Fig. 2b) throughout the forward and backward current processes, as shown in Fig. 4. Under the influence of reverse flow, water is distributed throughout the channel, making gas transport less obstructed and significantly reducing the voltage change and voltage decay rate of PST compared to DEA in the forward sweep. During the backward process, the membrane maintains its humidity, and combined with the water produced from the ORR reaction, more water droplets condense, resulting in higher voltage change and voltage decay rate for DEA compared to the forward process. However, PST still maintains similar compared to the forward sweep, as shown in Fig. 4a. The voltage stability index reflects transient voltage variations and assesses local flooding. The result in Fig. 4b shows that the voltage stability of DEA is higher than that of PST in both forward and backward, with the backward exhibiting higher stability than the forward. This is attributed to the localized accumulation of excess water, which is not uniformly distributed throughout the cell, thereby diminishing the stability of the output voltage.

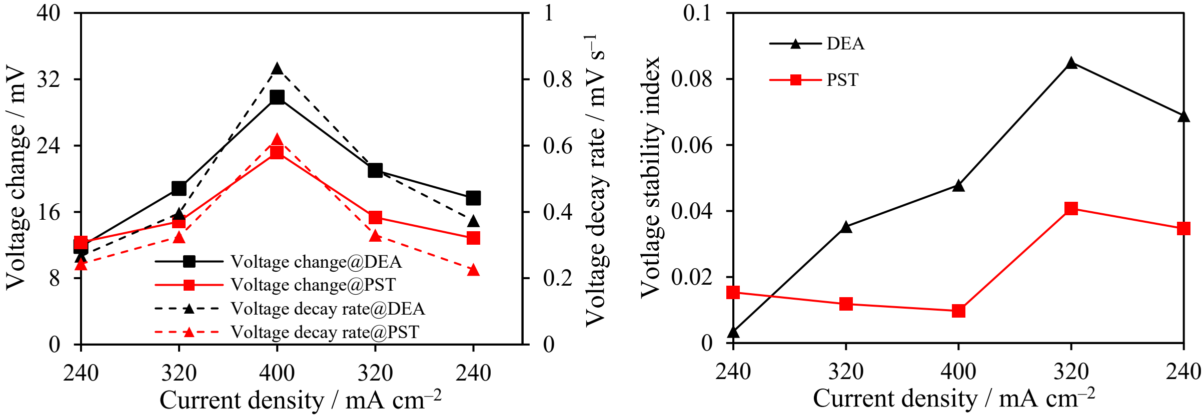

(a)

(b)

Fig. 4. Comparison of operating characteristics of PEMFC under DEA and PST at high current densities:
(a) Voltage change and voltage decay rate; (b) Voltage stability index.

3.2 Evaluating the effectiveness of purging interval

Fig. 5 illustrates the comparison of different purging intervals between DEA and PST at 320 mA cm^{-2}. Extending the purging interval results in a further decrease in outlet voltage. For short purging intervals, frequent purging continuously removes accumulated water, preventing significant condensation in the anode channel. This continuous forced convection clears the channel, thus improving PEMFC performance. However, if the purging interval is too short (lower than 10 s), water back diffusion to the anode is minimal, resulting in high ohmic resistance and increased fluctuation due to the continuous operation of the solenoid valve 2. Consequently, voltage degradation is severe with high voltage change. Nonetheless, the reverse flow effect prevents total membrane dehydration, leading to higher PST voltage, as shown in Fig. 5a. Additionally, under unstable conditions, the output voltage has not yet stabilized, resulting in a negative voltage decay rate and a high voltage stability index, as shown in Fig. 5b.

For long purging intervals, water back diffusion gradually leads to condensation in the porous electrode and gas channel, reducing the effective electrochemical reaction area and lowering PEMFC performance. However, the higher water concentration gradient hydrates the membrane better, resulting in less abrupt changes in ohmic resistance. Consequently, voltage change, voltage decay, and the voltage stability index for both DEA and PST configurations decrease significantly. Nonetheless, overly extended purging intervals cause water to accumulate into slugs that are difficult to remove, leading to flooding a nd increased voltage stability at 90 s.

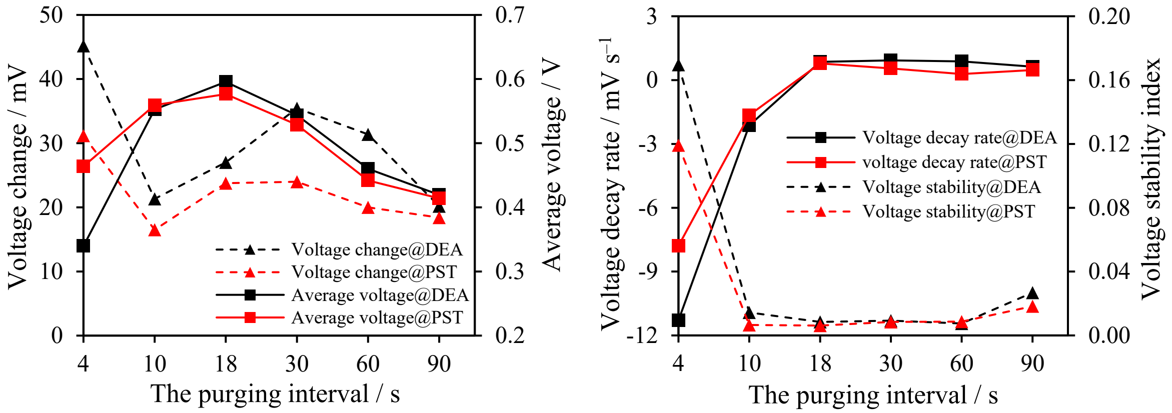

(a) (b)

Fig. 5. Comparison of operating characteristics of PEMFC under variable purging interval at 320 mA cm^{-2}: (a) Voltage change and average voltage; (b) Voltage decay rate and voltage stability index.

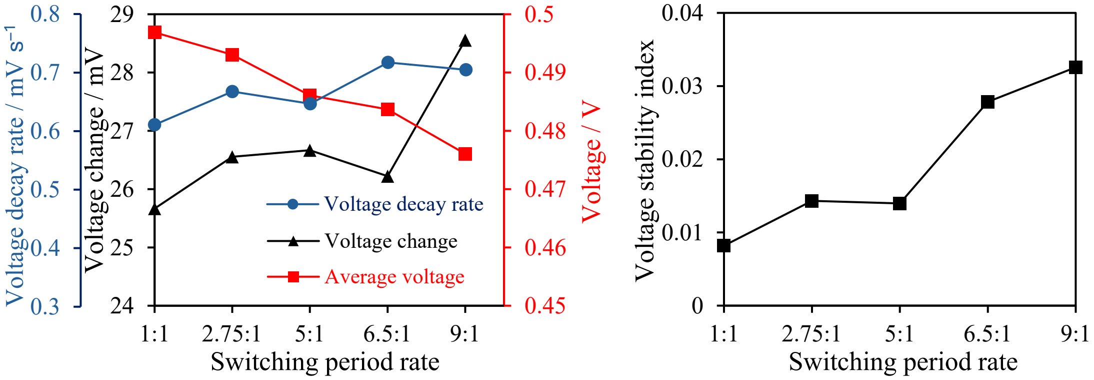

(a) (b)

Fig. 6. Switching period rate of solenoid valve 1 under PST configuration at 320 mA cm^{-2}: (a) Voltage change, voltage decay rate and output voltage; (b) Voltage stability index.

3.3 Evaluating the performance of switching rate of solenoid valve 1 in PST

Fig. 6 illustrates the impact of different switching period rates of solenoid valve 1 under PST operation at 320 mA cm^{-2}. The valve is set to open for 1, 2.75, 5, 6.5, 9 s, and close for 1 s. As shown in Fig. 6a, shorter switching periods enhance PEMFC performance by generating continuous reverse flow, which limits water accumulation, increases the output voltage, and reduces voltage change and decay rate. Conversely, longer switching periods slow the reverse flow, reduce the ability to redistribute water effectively, and apparently lead to water accumulation along the middle of the channel with larger droplet sizes, reducing the electrochemical area and decreasing output voltage. Fig. 6b shows the effect of switching period rates on the voltage stability index. The results indicate no significant difference from 1:1 to 5:1. However, lower switching rates result in decreased PEMFC stability, which can be explained by increased water accumulation, and raising the risk of flooding within the fuel cell channels.

4. Conclusions

In this study, the performance of a single PEMFC under DEA operating and PST operating was investigated. The parameters such as voltage difference, voltage change, voltage decay rate, and voltage stability were discussed and assessed. The main conclusions are as follows:

(1) The implementation of PST can effectively redistribute the uniformity of water in the anode channel, leading to significant reduction voltage fluctuations and the rate of voltage decay, thereby improving overall performance stability. However, the volume of water generated in a single cell is less substantial compared to that in a stack, resulting in insufficient membrane hydration. Consequently, the single-cell performance of PST is lower than that of DEA, with a particularly notable difference of 5.46% at 400 mA cm^{-2}.

(2) The fuel cell's performance during the backward process at high current densities deteriorates due to temporary flooding. However, enhanced membrane hydration at low current densities compared to the same current densities of forward process leads to a significant improvement in DEA performance, while PST performance remains stable.

(3) Under high loads, the purging interval parameter greatly impacts cell performance for both configurations. A longer purging interval results in more water accumulation in the cell and a more hydrated membrane, leading to better membrane stability but reduced performance. Conversely, a shorter interval affects cell stability and consumes more resources.

(4) Under the influence of varying switching period rates of solenoid valve 1 at high loads, single-cell performance decreases significantly with slower reverse flow rates. This reduction in water distribution capability decreases the active area of the cell, leading to notable increases in voltage fluctuation and voltage decay rate. However, cell stability is only significantly affected when the switching period rate exceeds 5 s.

Acknowledgments

This work was supported by the National Energy Technology Center (ENTEC) Thailand, with encouragement from King Mongkut's Institute of Technology Ladkrabang and Tokyo Institute of Technology.

References

[1] Gong M, Zhang X, Chen M, Tang J, Wang D. Proton Exchange Membrane Fuel Cell as an Alternative to the Internal Combustion Engine for Emission Reduction: A Review on the Effect of Gas Flow Channel Structures. Atmosphere. 2023;14(3):439.

[2] Agyekum EB, Ampah JD, Wilberforce T, Afrane S, Nutakor C. Research Progress, Trends, and Current State of Development on PEMFC–New Insights from a Bibliometric Analysis and Characteristics of Two Decades of Research Output. Membranes. 2022;12(11):1103.

[3] Madheswaran DK, Thangamuthu M, Gnanasekaran S, Gopi S, Ayyasamy T, Pardeshi SS. Powering the Future: Progress and Hurdles in Developing Proton Exchange Membrane Fuel Cell Components to Achieve Department of Energy Goals–A Systematic Review. Sustainability. 2023;15(22):15923.

[4] Ichikawa Y, Oshima N, Tabuchi Y, et al. Transient analysis of gas transport in anode channel of a polymer electrolyte membrane fuel cell with dead-ended anode under pressure swing operation. Journal of Power Sources. 2014;272:743–752.

[5] Chen J, Siegel JB, Stefanopoulou AG, Waldecker JR. Optimization of purge cycle for dead-ended anode fuel cell operation. International Journal of Hydrogen Energy. 2013;38(12):5092–5105.

[6] Kurnia JC, Sasmito AP, Shamim T. Advances in proton exchange membrane fuel cell with dead-end anode operation: A review. Applied Energy. 2019;252:113416.

[7] Do T-T, Devi N, Arpornwichanop A, et al. Study on the effect of cathode purge strategy on oxygen utilization of a proton exchange membrane fuel cell using oxygen. International Journal of Hydrogen Energy. 2024.

[8] Han I-S, Jeong J, Shin HK. PEM fuel-cell stack design for improved fuel utilization. International Journal of Hydrogen Energy. 2013;38(27):11996–12006.

[9] Mokmeli A, Asghari S. An investigation into the effect of anode purging on the fuel cell performance. Journal of Fuel Cell Science and Technology. 2010;35(17):9276–9282.

[10] Lee Y, Kim B, Kim Y. An experimental study on water transport through the membrane of a PEFC operating in the dead-end mode. International Journal of Hydrogen Energy. 2009;34(18):7768–7779.

[11] Meyer Q, Ashton S, Torija S, Gubler L, Steinfeldt N, Spolenak R. Nitrogen Blanketing and Hydrogen Starvation in Dead-Ended-Anode Polymer Electrolyte Fuel Cells Revealed by Hydro-Electro-Thermal Analysis. Electrochimica Acta. 2016;203:198–205.

[12] Hu Z, Yi Yu, Wang G, Li X, Li Y, Li H. Anode purge strategy optimization of the polymer electrode membrane fuel cell system under the dead-end anode operation. Journal of Power Sources. 2016;320:68–77.

[13] Yu J, Jiang Z, Hou M, Wang X, Guo S. Analysis of the behavior and degradation in proton exchange membrane fuel cells with a dead-ended anode. Journal of Power Sources. 2014;246:90–94.

[14] Chen B, Ke W, Luo M, Zhang Z, Zhang J. Operation characteristics and carbon corrosion of PEMFC (Proton exchange membrane fuel cell) with dead-ended anode for high hydrogen utilization. Energy. 2015;91:799–806.

[15] Chen B, Wang J, Yang T, Zhang Z, Luo M. Carbon corrosion and performance degradation mechanism in a proton exchange membrane fuel cell with dead-ended anode and cathode. Energy. 2016;106:54–62.

[16] Abbou S, Dillet J, Maranzana G, Minetti R, Maréchal F, Millet P. Local potential evolutions during proton exchange membrane fuel cell operation with dead-ended anode Part I: Impact of water diffusion and nitrogen crossover. Journal of Power Sources. 2017;340:337–346.

[17] Matsuura T, Chen J, Siegel JB, Stefanopoulou AG. Degradation phenomena in PEM fuel cell with dead-ended anode. International Journal of Hydrogen Energy. 2013;38(26):11346–11356.

[18] Jia Q, Zhang C, Deng B, Liu Y, Zuo P. Performance Improvement for Proton Exchange Membrane Fuel Cell Using Hydrogen Pressure Pulsation Approach. Journal of Fuel Cell Science and Technology. 2015;12(4):041012.

[19] Yang Y, Zhang X, Guo L, Li X, Chen H. Degradation mitigation effects of pressure swing in proton exchange membrane fuel cells with dead-ended anode. International Journal of Hydrogen Energy. 2017;42(38):24435–24447.

[20] Yang Y, Zhang X, Guo L, Li X, Chen H. Mechanisms of voltage spikes and mitigation strategies for proton exchange membrane fuel cells with dead-ended anode under pressure swing operation. International Journal of Hydrogen Energy. 2017;42(47):28578–28587.

[21] Huang Z, Zhao J, Jian Q. Voltage behavior improvement for proton exchange membrane fuel cell stack suffering fuel starvation. Energy Sources. 2019;45(3):6500–6514.

[22] Zhao J, Jian Q, Huang Z. Experimental and theoretical study on improving the operating characteristics of an open-cathode PEMFC stack by generating periodic disturbances at anode. Energy Conversion and Management. 2019;196:1433–1444.

[23] Zhao J, Jian Q, Huang Z, Wang Y, Li X. Experimental study on water management improvement of proton exchange membrane fuel cells with dead-ended anode by periodically supplying fuel from anode outlet. Journal of Power Sources. 2019;435:226–234.

[24] Zhao J, Jian Q, Huang Z. Visualization study on enhancing water transport of proton exchange membrane fuel cells with a dead-ended anode by generating fluctuating flow at anode compartment. Energy Conversion and Management. 2020;206:112477.

[25] Yang Y, Zhang X, Guo L, Li X, Chen H. Local degradation in proton exchange membrane fuel cells with dead-ended anode. Journal of Power Sources. 2020;477:229021.

[26] Lin H, Jian Q, Bai X, Zhao J, Huang Z. Mitigating performance deterioration analysis of VC-PEMFC with dead-ended anode by pulsation fuel supplying mode. International Journal of Hydrogen Energy. 2023;48(27):10144–10159.

[27] Zhao J, Zhou C, Han J, Huang Z, Jian Q. Numerical analysis of improved water management of open-cathode proton exchange membrane fuel cells with a dead-ended anode by pulsating flow. International Journal of Hydrogen Energy. 2023;48(44):16858–16874.

[28] Song Y, Zhang C, Jia Q, Zhao J, Huang Z. Novel closed anode pressure-swing system for proton exchange membrane fuel cells. International Journal of Hydrogen Energy. 2020;45(35):17727–17735.